Journal of Inclusion Phenomena and Macrocyclic Chemistry **50**: 219–225, 2004.
© 2004 *Kluwer Academic Publishers. Printed in the Netherlands.*

Preparation and Investigation of Inclusion Complexes Containing Gemfibrozil and DIMEB

HASSAN BIN HASSAN*, MIHÁLY KATA, ISTVÁN ERŐS and ZOLTÁN AIGNER
Department of Pharmaceutical Technology, University of Szeged, H-6720 Eötvös utca 6, Hungary

(Received: 2 February 2004; in final form: 28 June 2004)

Key words: dissolution, FTIR, gemfibrozil, heptakis-2,6-di-*O*-methyl-β-cyclodextrin, inclusion complexes, membrane diffusion, thermoanalytical investigations

Abstract

Gemfibrozil (GEM) is a xylyloxi-valeric acid derivative with an antilipaemic effect. This molecule has very poor water solubility, and the ability of different cyclodextrins (CDs) to form inclusion complexes was therefore tested. Primarily heptakis-2,6-di-*O*-methyl-β-cyclodextrin (DIMEB) was found to increase the solubility. The preparation of the complex in solid form for characterization was successful by means of physical mixing, kneading, spray-drying and ultrasonic treatment. The dissolution and *in vitro* membrane diffusion of the products were investigated. The *n*-octanol/water partition coefficients were determined for pure GEM and the DIMEB inclusion product, and the interactions leading to complex formation between the components of the products were examined by thermoanalytical methods and FTIR spectrophotometric analysis.

Introduction

Gemfibrozil (GEM) is a serum lipid-regulating agent which decreases the serum levels of triglycerides and very low-density lipoprotein cholesterol, and increases that of high-density lipoprotein cholesterol [1, 2]. GEM is strongly bound to the protein plasma (albumin) and 70% of the administered dose is excreted in the urine [1]. Complex formation may result in an increased water solubility, increased chemical and physical stability, or an increased bioavailability of the drug molecule [3, 4]. The present study had the aim of an investigation of the interactions between GEM and various CDs and their effects on the GEM solubility properties, with a view to improving the bioavailability of GEM, and therefore decreasing its dose and side-effects [5–8].

Experimental

Materials

Gemfibrozil (GEM): 2,2-dimethyl-5-(2,5-xylyloxy)valeric acid (Plantex Chemicals, Israel, API Division Teva Group) (Figure 1), α-CD, β-CD, γ-CD, 2-hydroxypropyl-β-CD (HP-β-CD), hydroxybutenyl-β-CD (HBU-β-CD), randomly methylated-β-CD (RAMEB), heptakis-2,6-di-*O*-methyl-β-CD (DIMEB) (Cyclolab R & D Laboratory Ltd., Budapest, Hungary); Captisol® (CyDex, Inc., USA); other chemicals (Reanal Co., Budapest, Hungary).

Apparatus

USP dissolution apparatus, type DT [9]; kneading mixer, type LK5 (Erweka Apparatebau GmbH, Heusenstamm, Germany); Grant XB2 ultrasonic bath (Grant Instruments Ltd., Cambridge, UK); Unicam UV2/Vis spectrometer (Unicam Ltd., England); Sartorius membrane apparatus (Sartorius-Membranfilter GmbH, Germany); Derivatograph-C computing thermal analysis system (MOM, Budapest, Hungary); Mettler Toledo DSC 821^e thermal analysis system with the STAR^e thermal analysis program, version 6.0 (Mettler Inc., Schwerzenbach, Switzerland); Dataphysics OCA20 (Dataphysics Inc., GmbH, Germany); Büchi Mini Dryer B-191 (Switzerland); AVATAR 330 FT-IR spectrometer (Thermo Nicolet, USA); Specac hydraulic press (Specac Inc., USA); Hitachi 2400S scanning electron microscope (Hitachi Ltd., Japan).

Preliminary experiments

Preliminary experiments were carried out to ascertain which CD derivative most increases the solubility of the active ingredient. Mixtures of 0.02 g GEM and 0.20 g of the different CDs were diluted to 20.0 g with distilled water and then stirred for 10 min with a magnetic stirrer. The suspension systems were filtered through

* Author for correspondence. E-mail: hassan@pharma.szote.u-szeged.hu

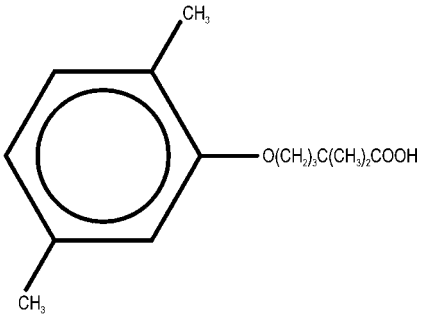

Figure 1. Chemical structure of gemfibrozil.

Table 1. Influence of CD derivatives on the solubility of gemfibrozil (μg mL^{-1})

Gemfibrozil (GEM)	29.10
GEM + α-CD	31.39
GEM + β-CD	49.62
GEM + γ-CD	253.44
GEM + HP-β-CD	212.71
GEM + HBU-β-CD	284.84
GEM + RAMEB	330.63
GEM + DIMEB	655.44
GEM + Captisol®	251.91

filter papers and the UV spectra were recorded. A system without CD was used as control. DIMEB exerted the highest solubility-increasing effect on the active ingredient, and accordingly this compound was used for further examinations (Table 1).

The absorption maximum of the active ingredient was at 276 nm. The calibration curve was obtained in the concentration interval 0–150 μg mL^{-1}, where the equation was found to be $A = 0.00653c$ for both of the calibration plots, prepared either with or without DIMEB.

Preparation of products

Products were prepared in four different molar ratios (GEM : CD molar ratio = 2:1, 1:1, 1:2 and 1:3). *Physical mixtures*: the pure drug and CD were mixed in a mortar and sieved through a 100 μm sieve. *Kneaded products*: physical mixtures of the drug and DIMEB were mixed (Erweka LK5) with the same quantity of a solvent mixture of ethanol + water (1:1). They were kneaded until the bulk of the solvent mixture had evaporated. After this, they were dried at room temperature and were then pulverized and sieved through a 100 μm sieve. *Spray-dried products*: the physical mixtures of GEM and DIMEB were dissolved in 50% ethanol. The spray-dried products were obtained by using a Büchi Mini Dryer B-191, at 75 °C inlet temperature with compressed air flow: 800 L min^{-1} and nozzle diameter: 0.5 mm. The aspirator rate was 75–80%, and the pump rate was 3–7% [10]. *Products prepared by ultrasonic treatment*: physical mixtures with different molar ratios of GEM and DIMEB were dissolved in 50% ethanol and mixed to obtain clear solutions, then placed in the ultrasonic apparatus for 1 h, dried at room temperature, pulverized and sieved through a 100 μm sieve. Products were stored under normal conditions at room temperature in well-closed glass containers.

Phase solubility

Solubility measurements were conducted in distilled water pH (6.2 ± 0.1) according to Higuchi and Connors [11]. Excess GEM was added to aqueous solutions containing various concentrations of DIMEB (0–200 mM), which were then stirred at room temperature until equilibrium was reached (≈48 h). After filtration, the concentration of GEM was measured spectrophotometrically. The stability constant (K_s) was determined from the phase solubility diagram by using the equation of Higuchi and Connors, on the assumption that a complex with a stoichiometric ratio of 1:1 was formed in the initial step.

Dissolution studies

A modified paddle USP dissolution apparatus was used [9] to examine 20 mg samples of pure GEM or products containing 20–100 mg of drug in 100 mL of simulated gastric medium (pH = 1.1 ± 0.1): 1N HCl 94.00 g, NaCl 0.35 g, glycine 0.50 g in 1000 mL of distilled water; or simulated intestinal medium (pH = 7.0 ± 0.1): $Na_2HPO_4 \cdot 2H_2O$ 14.4 g, KH_2PO_4 7.1 g in 1000 mL of distilled water. The basket was rotated at 100 rpm, the sampling volume was 5.0 mL, and the temperature was 37 ± 1 °C. After filtration and dilution, the GEM contents of the samples were determined spectrophotometrically at 276 nm.

Membrane diffusion

Stricker's Sartorius apparatus was used [12, 13]. Measurements were performed on 100.0 mL of simulated gastric or intestinal medium in simulated plasma (pH = 7.5 ± 0.1): $Na_2HPO_4 \cdot 2H_2O$ 20.5 g, KH_2PO_4 2.8 g in 1000 mL of distilled water. 20 mg samples of drug or products containing 20 mg of GEM were placed in the donor phase in all cases. The artificial membrane was of cellulose acetate (pore size 3 μm, diffusion surface 40 cm^2). The temperature was 37.5 ± 1.5 °C. Five milliliters samples were taken five times (after 30, 60, 90, 120 and 150 min) and their GEM contents were determined spectrophotometrically after filtration. The amount of diffused active agent and the diffusion constant K_d were calculated in the linear part of the diffusion curves:

$$K_d = \frac{c_{II2} - c_{II1}}{T_2 - T_1} \cdot \frac{1}{c_{I0}} \cdot \frac{V_{II0}}{F} [\text{cm min}^{-1}],$$

where c_{IIx} is the corrected drug concentration in phase II at time T_x (mg mL^{-1}); V_{II0} is the volume of aqueous phase II at time T_0 (100 mL); F is the surface area of the membrane (cm^2); T_x is time (min); and c_{I0} is the theoretical initial drug concentration in phase I (mg mL^{-1}) [13, 14].

Determination of the n-octanol/water partition coefficient

The *n*-octanol–water system is a model that is widely used to investigate diffusion across biological membranes [15]. GEM or products containing GEM were suspended in water-saturated *n*-octanol and in *n*-octanol-saturated water. Further drug or CD products was added to these systems during continuous stirring until the excess drug appeared in suspended form. After filtration, the saturated solution was diluted with *n*-octanol-saturated water or water-saturated *n*-octanol, and the drug content was determined spectrophotometrically.

Thermoanalytical methods

The CDs are capable of forming inclusion complexes with a high number of drugs by taking up a whole drug molecule, or some part of it, into the cavity [16]. The complex formation between the components of the products was examined by means of thermoanalytical methods [17]. Approximately 2–5 mg of pure drug or product (in the case of DSC studies) or 50 mg of powder (in the case of TG, DTG, and DTA) was examined in the temperature range 25–300 °C. The heating rate was 5 °C min^{-1}, and the flow rate of argon gas during the DSC measurements was 167 mL min^{-1} (10 L h^{-1}).

The uncomplexed guest percentages were estimated semiquantitatively from the DSC curves by using the following equation:

$$\text{uncomplexed} - \text{guest}\% = \frac{\Delta H_i}{\Delta H_0 \cdot c} \cdot 10^4,$$

where ΔH_i is the normalized integral data on the product; ΔH_0 the normalized integral data on the active ingredient; and c is the percentage active ingredient in the product.

Fourier transform infrared spectroscopy (FTIR)

The FTIR spectra of the GEM and the solid products (in KBr disks) were recorded on an AVATAR 330 FTIR in the interval 450–4000 cm^{-1}. The pressure was 10 tons, and the diameter of the pressings was 13 mm.

Results

Phase solubility studies

The phase diagrams, i.e., the solubility curves, can be divided into two major categories (Higuchi and Connors, 1965). Type *A* solubility curves are obtained when the apparent solubility of the substrate increases with increasing ligand concentration throughout the entire concentration range. A linear relationship is designated as of A_L type, while the A_P and A_N curves exhibit positive and negative curvature, respectively. In this case, we obtained a freely soluble complex form, where the solubility limit was determined only by the solubility of the CD. The initial linear ascending part of a solubility diagram is generally ascribed to the formation of a 1:1 complex when the slope is less than 1. When the complex is more soluble than that the free guest, but its solubility limit can be reached within the CD concentration range, the guest concentration first increases from the aqueous solubility of the guest until the point where the solubility limit of the complex is reached [8].

Figure 2 shows an A_L-type phase solubility equilibrium diagram for the GEM/DIMEB system in water at 25 °C. The solubility of GEM increased linearly in the presence of this CD derivative.

The apparent stability constant (K_c) can be calculated from the slope and intercept of the initial linear portion of the diagram as follows:

$$K_c = \frac{\tan \alpha}{S_0(1 - \tan \alpha)},$$

where S_0 is the solubility of GEM in the absence of CD. K_c was calculated to be 2.755 ± 0.047 M^{-1}.

Dissolution examinations

GEM dissolves sparingly at pH 1.1: only 2.66 mg/100 mL dissolved during the 2-h investigation period. The solubility is better at pH 7.0, as a result of its chemical nature: 38.01 mg dissolves in 100 ml acceptor phase in 2 h.

The dissolution of the CD-containing products was in all cases better than that of the pure drug. On increase of the CD content, the solubility increases further, which is well manifested in the case of the physical mixtures. A

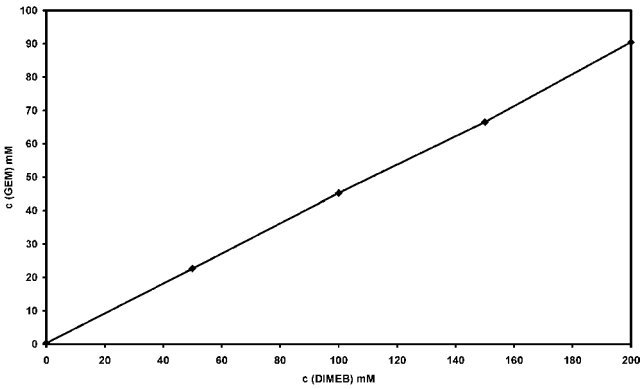

Figure 2. Phase solubility diagram of GEM with DIMEB in water at 25 °C.

Table 2. Summarized dissolution results of GEM and products (mg 100 mL^{-1})

Product		Simulated gastric medium				Simulated intestinal medium			
		10th min	SD	120th min	SD	10th min	SD	120th min.	SD
GEM		1.34	0.13	2.66	0.43	14.13	3.94	38.01	1.68
Physical mixture	2:1	5.42	0.21	6.20	0.24	59.59	7.06	90.15	3.76
	1:1	8.26	0.26	9.12	0.11	74.56	2.68	98.39	2.33
	1:2	12.24	0.34	14.39	0.30	92.13	8.79	104.05	12.39
	1:3	13.57	0.93	18.11	0.67	95.37	5.49	99.57	4.41
Kneaded product	2:1	2.84	0.13	4.14	0.29	51.27	9.24	141.08	4.71
	1:1	11.27	0.48	10.32	0.16	169.73	9.53	175.86	12.81
	1:2	99.71	1.64	90.17	3.00	202.19	22.53	201.70	8.66
	1:3	101.55	4.45	104.73	2.64	192.77	4.84	198.23	2.82
Spray-dried product	2:1	7.08	0.21	10.51	1.23	55.59	6.99	108.40	22.68
	1:1	46.78	5.25	43.97	3.20	160.19	3.91	186.55	10.36
	1:2	100.56	2.24	93.63	2.18	187.68	13.12	192.81	10.67
	1:3	107.16	2.12	109.58	1.51	190.60	1.88	195.22	3.44
Ultrasonic treatment product	2:1	22.34	0.80	40.02	2.35	65.28	5.29	130.46	6.66
	1:1	60.38	1.65	85.89	5.06	137.87	7.55	193.22	3.00
	1:2	191.79	6.78	193.17	1.36	187.14	3.40	193.14	2.40
	1:3	187.23	2.57	200.18	2.84	183.22	4.81	192.65	4.00

7-fold solubility increase was measured for the 1:3 product.

Similar phenomena were observed for the kneaded, spray dried and ultrasonic treatment products: the dissolved drug amount increased with increasing CD content. The total drug amount dissolved in the early stages of the investigation at higher CD ratios (1:2 and 1:3). It was also typical that the saturation concentration was reached in 5–10 min for the kneaded and spray-dried products, while the ultrasonic treatment products needed 30 min to reach the same state.

The effect of the presence of the CD was not so expressed when measurements were made in simulated intestinal medium. The solubility was increased in all cases as compared with pure GEM, but the differences between the different products were not so significant. A 3–6-fold solubility increase was measured, depending on the preparation methodology. Table 2 contains the summarized dissolution results of GEM and all of the products. Some of the products dissolved totally in the small volume of acceptor phase, in spite of the increased active agent content of the product. Therefore, the saturation concentration was determined for all of the products.

Figure 3 shows these results for simulated gastric medium, while Figure 4 illustrates the data measured in simulated intestinal medium. Especially the 1:2 and 1:3 spray dried and ultrasonicated products may be emphasized (520-fold solubility increase for the 1:2 US in simulated gastric medium). The preparations made by

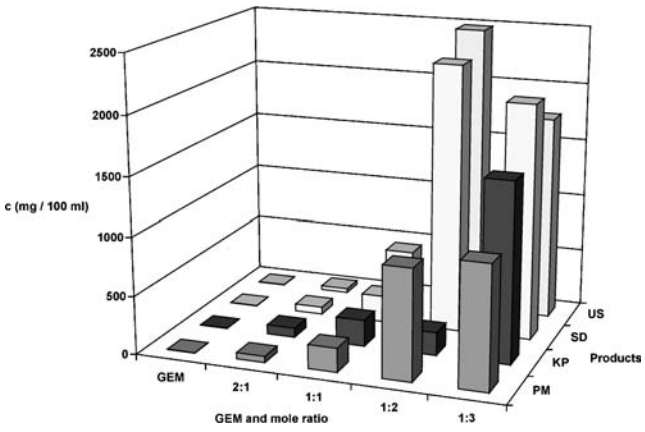

Figure 3. Saturated concentrations of products and GEM in simulated gastric medium. PM – physical mixture; KP – kneaded product; SD – spray-dried product; US – ultrasonic treatment product.

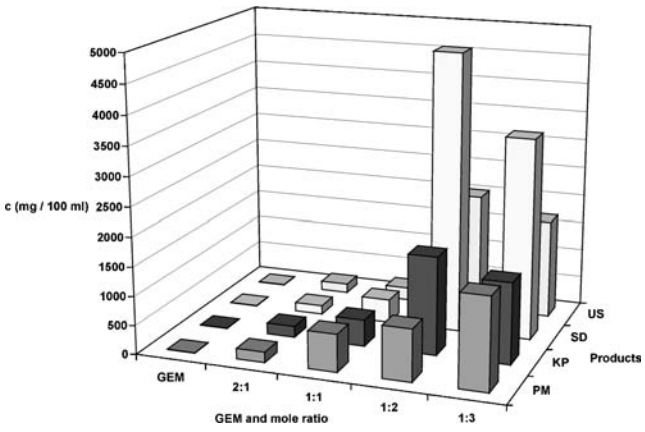

Figure 4. Saturated concentrations of products and GEM in simulated intestinal medium. PM – physical mixture; KP – kneaded product; SD – spray-dried product; US – ultrasonic treatment product.

Table 3. Diffusion constants (K_d) of GEM and products from simulated gastric medium

Products		$K_d(10^{-3})$ [cm/min]	SD
GEM		0.640	0.069
Physical mixture	2:1	1.526	0.043
	1:1	1.529	0.853
	1:2	3.228	0.172
	1:3	3.616	0.163
Kneaded product	2:1	1.547	0.283
	1:1	1.934	0.043
	1:2	4.308	0.746
	1:3	4.909	0.549
Spray-dried product	2:1	1.043	0.202
	1:1	2.631	0.086
	1:2	3.966	0.420
	1:3	4.914	0.223
Ultrasonic treatment product	2:1	2.077	0.197
	1:1	3.775	0.219
	1:2	1.934	0.034
	1:3	5.438	0.557

Table 5. *n*-octanol/water partition coefficients of GEM and products

		$c_{n\text{-octanol}}$ (μg/ml)	c_{water} (μg/ml)	c_0/c_w
GEM		658.499	98.009	6.719
Physical mixture	2:1	594.181	214.395	2.771
	1:1	393.568	490.046	0.803
	1:2	407.351	5528.330	0.074
	1:3	309.341	18483.920	0.017
Kneaded product	2:1	332.312	811.638	0.409
	1:1	366.003	2557.427	0.143
	1:2	261.868	3292.496	0.080
	1:3	243.491	4287.902	0.057
Spray-dried product	2:1	915.773	1439.509	0.636
	1:1	162.328	796.325	0.204
	1:2	618.683	3797.856	0.163
	1:3	686.064	3016.845	0.227
Ultrasonic treatment product	2:1	1009.188	137.825	7.322
	1:1	105.666	842.266	0.125
	1:2	185.298	3797.856	0.049
	1:3	140.888	7442.573	0.019

the spray-drying method gave the best results in simulated intestinal medium (a 716-fold solubility increase at a ratio of 1:2).

Membrane diffusion results

1.4 mg of the pure drug diffused through the membrane into simulated gastric medium during 150 min under *in vitro* conditions. We experienced increased diffusivity with increasing CD content. A 3.2-fold increase was measured for the physical mixtures, a 4-fold one for the kneaded and spray-dried products, and a 5.4-fold increase in diffusivity for the ultrasonic treatment products.

The products displayed no difference in diffusivity as compared with the pure drug when measurements were carried out in simulated intestinal medium. The diffused drug amount was not dependent on the composition of the products or on the preparation method used. Eight milligram GEM was able to diffuse during 150 min. The last part of the diffusion curves exhibited a saturated character, as a consequence of the increased diffused drug amount. This is the explanation of the significant differences in the values of the diffusion rate constants. Therefore, the linear part (between 30 and 90 min) of the curves was used to calculate the diffusion rate constants. Tables 3 and 4 list these diffusion rate constants.

Table 4. Diffusion constants (K_d) of GEM and products from simulated intestinal medium

Products		$K_d(10^{-3})$ [cm/min]	SD
GEM		6.225	0.189
Physical mixture	2:1	6.742	0.532
	1:1	7.301	1.187
	1:2	6.351	0.184
	1:3	7.112	1.414
Kneaded product	2:1	7.439	0.544
	1:1	6.692	0.939
	1:2	7.036	1.286
	1:3	7.581	1.582
Spray-dried product	2:1	7.648	0.441
	1:1	7.614	3.935
	1:2	6.772	0.982
	1:3	7.234	0.977
Ultrasonic treatment product	2:1	12.536	1.834
	1:1	7.474	0.506
	1:2	7.144	1.419
	1:3	7.215	1.543

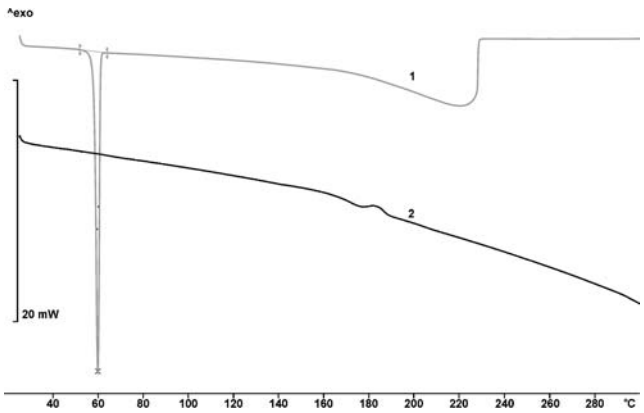

Figure 5. DSC curves of GEM (1) and DIMEB (2).

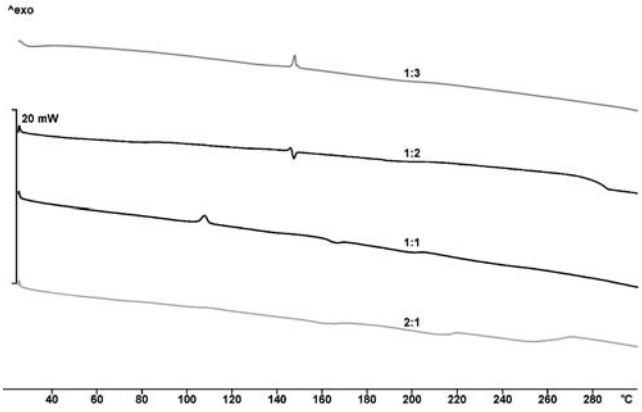

Figure 6. DSC curves of spray-dried products.

Results of n-*octanol/water partition coefficient*

GEM has a high partition coefficient as it has poor water solubility and a high affinity for *n*-octanol. All the partition coefficients of the products were lower than that of the pure drug. The aqueous solubility increased with increasing CD content, in parallel with decreasing *n*-octanol solubility. The relevant results are shown in Table 5.

Thermoanalytical results

A distinction can be made between surface adsorption and inclusion complex formation by means of thermoanalytical methods. The presence of an inclusion complex is shown indirectly by changes relative to the non-complexed free drug.

Complex formation can be easily followed by evaluation of the DSC curves of the products. Figure 5 shows the DSC curves of the pure drug and DIMEB alone. A sharp endothermic peak can be distinguished at 59.25 °C in the curve of the drug, which can be identified from the literature data as its melting point. The melted drug evaporated on further increase of temperature, this process being enhanced by the open container and also by the argon gas flow. The total drug amount evaporated at 230 °C; after this, only the baseline is seen.

The fact of evaporation was confirmed by studying the TG curve of the active agent: a continuous mass loss was measured in the above mentioned temperature range.

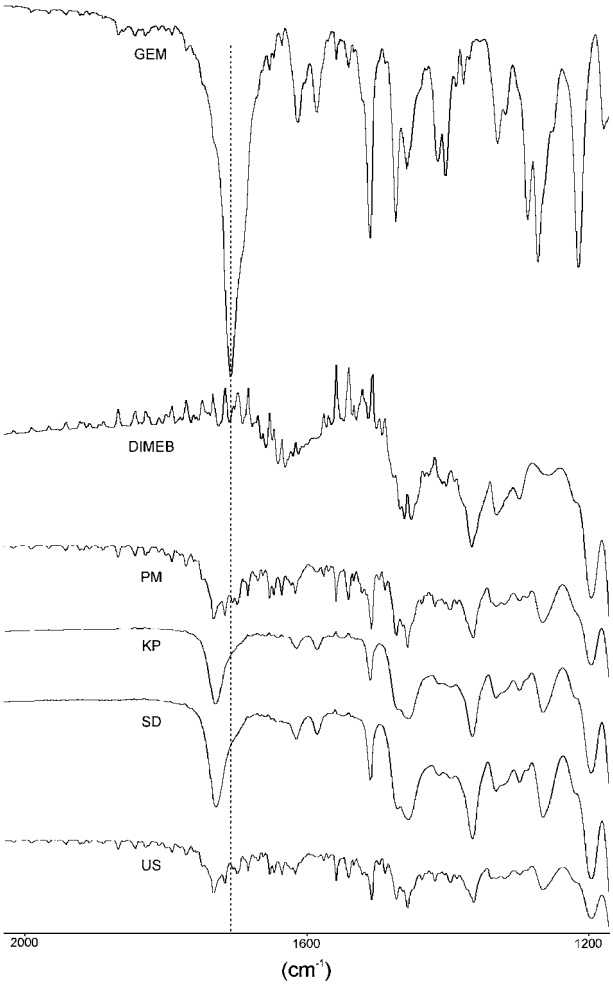

Figure 7. FTIR spectra of DIMEB, GEM, and 1:1 products. PM – physical mixture; KP – kneaded product; SD – spray-dried product; US – ultrasonic treatment product.

There is no wide endothermic peak in the DSC curve of DIMEB under 100 °C which would be caused by the moisture content of the complex-forming agent; the moisture content of this CD derivative was under 1%, as measured by TG. The small exothermic and endothermic peaks between 170 and 190 °C are caused by CD impurities. The low moisture content of DIMEB is advantageous as the endothermic peak caused by moisture would disturb the study of the drug melting point.

The endothermic peak reflecting the melting point of the drug is well manifested at all molar ratios of the physical mixtures. The integrated area and the normalized integral are proportional to the drug content of the individual product; on the basis of these data, we can calculate a partial complex formation of 20–30% [18].

As concerns the products made by the other preparation methods, only the 2:1 kneaded and ultrasonic treatment products displayed a partial complex formation of 80–90%. No melting endothermic peaks were observed at other molar ratios of the kneaded and ultrasonic treatment products, indicating complete complex formation. Figure 6 shows the DSC curves of spray-dried products as an example.

FTIR results

Complex formation may be demonstrated by IR spectroscopy in some cases, but this method is of limited use in the investigation of CD inclusion complexes. The characteristic bands of the CD, representing the overwhelming part of the complex, are scarcely influenced by complex formation. The bands due to the included part of the guest molecule are generally shifted or their structures are altered, but the mass of the guest molecule does not exceed 5–15% of the host. The IR spectroscopic studies of such CD complexes which have a carbonyl group-bearing guest are reported. The carbonyl bands are well separated (about 1680–1700 cm^{-1}), which are significantly shifted and overlap on CD complexation [8].

The Figure 7 presents the FTIR spectra of GEM, DIMEB and the 1:1 products. The major peak at 1708 cm^{-1} of the carbonyl C=O stretching is the important characteristic of GEM. A shift of this to 1727–1733 cm^{-1} was observed for all the products. This suggests a modification of the electronic environment of the characteristic molecular group of GEM, which means inclusion complex formation in the solid state. The FTIR results confirmed the observations made from the DSC curves.

Conclusions

DIMEB proved to be the most adequate CD with which to increase the aqueous solubility of poorly soluble GEM. The phase solubility of the active agent was linear in the investigated CD concentration range. 16 different products were prepared from the drug and the complex-forming agent, all of them exhibited better dissolution data than those for the drug alone. A more than 500–700-fold solubility increase was observed during the saturation concentration measurements. A 3–5-fold increase was measured during the *in vitro* membrane diffusion studies with simulated gastric medium, whereas no significant difference was detected in simulated intestinal medium. Complexation with DIMEB decreased the *n*-octanol/water partition coefficient considerably.

Complex formation was proved by thermoanalytical and FTIR measurements in several compositions made by different preparation methods.

The 1:2 kneaded and spray-dried products were selected for further research on the basis of these investigations. The preparation of solid dosage forms (film tablets and capsules) and also *in vivo* availability and adverse effect measurements belong among our future tasks.

Acknowledgement

This work was supported by the Hungarian National Scientific Research Fund (OTKA).

References

1. *Gyógyszer Kompendium 2002* (*Pharma Compendium 2002*), Medi-Media Információs Kft., Budapest (2002), pp. 713, 906.
2. *The Merck Index*, 11th edn., Merck & Co., Inc. Rathway, NJ (1989), p. 686.
3. J. Szejtli: In V.F. Smolen and L.A. Ball (eds.), *Controlled Drug Bioavailability*, Vol. 3, J. Wiley and Sons, New York (1985), p. 365.
4. D.O. Thompson: *Crit. Rev. Ther. Drug Car. Syst.* **14**, 1 (1997).
5. J. Szejtli: *Cyclodextrin Technology*, Kluwer, Dordrecht/Boston/London (1988).
6. J. Szejtli: *Cyclodextrins and their Inclusion Complexes*, Akadémiai Kiadó, Budapest (1982), p. 33.
7. M. Kata, M. Schauer and B. Selmeczi: *Acta Pharm. Hung.* **61**, 23 (1991).
8. H.-K. Frömming and J. Szejtli: *Cyclodextrins In Pharmacy*, Kluwer, Dordrecht (1994), pp. 94, 105.
9. USP: 23rd edn., US Pharm. Conv. Inc., Rockville, MD (1994).
10. Z. Aigner, M. Kata: *S.T.P. Pharm. Sci.* **9**, 279 (1999).
11. T. Higuchi and K.A. Connors: *Adv. Anal. Chem. Instr.* **4**, 117 (1965).
12. H. Stricker: *Pharm. Ind.* **31**, 794 (1969).
13. *Booklet of Sartorius Resorption Model,* SM 16750, Göttingen (1976), p. 15.
14. H. Stricker: *Pharm. Ind.* **33**, 157 (1971); **35**, 13 (1973).
15. J. Arct and E. Starzyk: *SÖFW-Journal* **129**, 2 (2003).
16. T. Laftsson, J. Baldvinsdottir, H. Fridriksdottir, and A.M. Sigurdardottir: 53rd FIP Congress, TOKYO, p. 7. (1995).
17. F. Giordano, Cs. Novák, and J.R. Moyano: *Thermochim. Acta* **380**, 123 (2001).
18. Z. Aigner, I. Benz, and M. Kata: *J. Incl. Phenom.* **20**, 241 (1995).